Viscoelastic deformation of a dielectric elastomer membrane subject to electromechanical loads

Huiming Wang,[1,2] Ming Lei,[1] and Shengqiang Cai[3,a)]
[1]*Department of Engineering Mechanics, Zhejiang University, Hangzhou 310027, People's Republic of China*
[2]*Soft Matter Research Center (SMRC), Zhejiang University, Hangzhou 310027, People's Republic of China*
[3]*Department of Mechanical and Aerospace Engineering, University of California, San Diego, La Jolla, California 92093, USA*

(Received 20 March 2013; accepted 13 May 2013; published online 3 June 2013)

Inhomogenous viscoelastic deformation is analyzed for a membrane of dielectric elastomer mounting on a rigid circular ring and subject to a combination of pressure and voltage. The membrane is assumed to be capable of large deformation, and the viscoelasticity of the membrane is represented by a nonlinear spring-dashpot model. It is found that when the applied pressure and voltage are small, the dielectric membrane gradually evolves to an equilibrium state. While if the applied pressure and voltage are large, the membrane cannot reach equilibrium state and electromechanical instability may happen with the time. The evolution of different fields in the dielectric elastomer membrane and its profile are calculated in this article. The model can be potentially used to explore time dependent behaviors of dielectric elastomeric devices. © *2013 AIP Publishing LLC*. [http://dx.doi.org/10.1063/1.4807911]

I. INTRODUCTION

Dielectric elastomer consists of a thin and soft membrane and two compliant electrodes coated on its surfaces. When subject to a voltage, the membrane of dielectric elastomer reduces thickness and expands area. In 2000, Pelrine *et al.* reported that the electrically actuated strain in the dielectric elastomers can reach greater than 100%.[1] Since then, large deformation and kinetic processes in dielectric elastomers have been intensively studied.[2–14] More recently, by careful loading design, Huang *et al.* experimentally realized a very large voltage-actuated strain, up to 488% expansion in area.[15] Li *et al.* observed giant voltage-induced expansion in dielectric elastomer through harnessing the snap-through instability.[16] In addition to large deformation, dielectric elastomers have many other attractive features, such as fast response, low cost, light weight, high energy density, and so on. Nowadays, dielectric elastomers have been developed as diverse intelligent devices, such as actuators, tunable lens, energy harvesters, and refreshable displays.[17–22]

Most dielectric elastomers are rubbery polymer. The behaviors of these polymers are usually stretch-rate dependent. For instance, in uniaxial tension tests, the stress-stretch curves can strongly depend on stretch-rate.[23,24] Recent experiments have also shown that the fracture energy of VHB (a kind of acrylic foam tapes fabricated by 3M Company), the most extensively investigated dielectric elastomer material, also changes dramatically with stretch-rate.[25] These stretch-rate dependent behaviors are usually interpreted as the consequence of the viscoelasticity of the polymers,[26] which may have significant influence on the performances of dielectric elastomer devices.[27,28] For example, as demonstrated by Plante and Dubowsky, at high velocities, the viscoelasticity of the elastomer can reduce the actuating forces of the devices.[29]

To investigate the interplay of viscoelasticity and electric field in a dielectric elastomer membrane undergoing inhomogeneous deformation, a theoretical model is developed in this article. Based on the model, the time-dependent behavior of a dielectric elastomer is calculated numerically. The evolution of the physical fields and the profiles of the elastomeric membrane with the time are also presented.

II. GOVERNING EQUATIONS AND BOUNDARY CONDITIONS

Figure 1 illustrates the mechanical model of a dielectric elastomer membrane. In the undeformed state, the membrane is of a flat circular shape with radius A and thickness H, Fig. 1(a). The membrane is then homogeneously prestretched and clamped on the rigid ring of radius a, Fig. 1(b). In the deformed state, the membrane is inflated by a fixed pressure p and a fixed voltage Φ across its thickness. Let the z-axis coincide with the axis of symmetry and r-axis coincide with the radial direction. The plane $z = 0$ locates at the plane of rigid ring. Consider the particle R in the undeformed state. It moves to a new place $(r(R,t), z(R,t))$ in the deformed state, Fig. 1(c). Here, t is the time variable. The longitudinal stretch is defined as $\lambda_1 = \mathrm{d}l/\mathrm{d}R$ and the latitudinal stretch $\lambda_2 = r/R$. Here, $\mathrm{d}l$ is the length of the material element in the longitudinal direction in the deformed state. In this article, the dielectric elastomer is modeled as the viscoelastic material. Therefore, all the physical fields are time dependent in spite of the constant loadings. Denote $\theta(R,t)$ as the slope of the membrane at the particle R. Then we have $\mathrm{d}r = \mathrm{d}l\cos\theta$ and $\mathrm{d}z = -\mathrm{d}l\sin\theta$ and so that

$$\frac{\partial r}{\partial R} = \lambda_1 \cos\theta, \tag{1}$$

$$\frac{\partial z}{\partial R} = -\lambda_1 \sin\theta. \tag{2}$$

a)email: shqcai@ucsd.edu

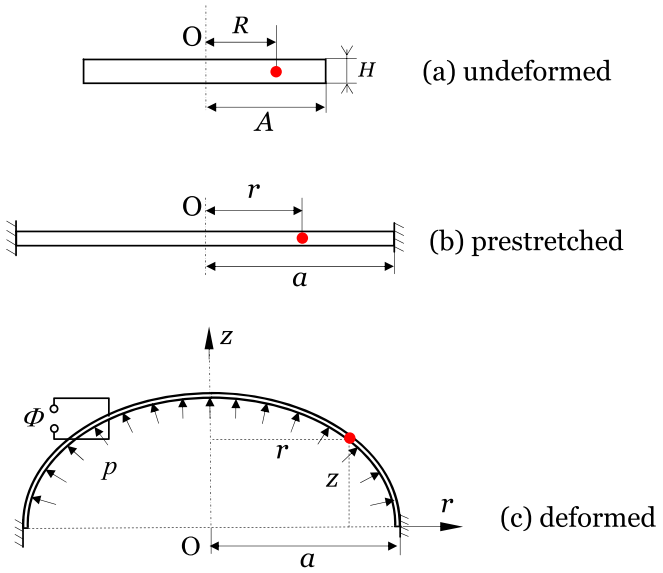

FIG. 1. Mechanical model of the dielectric elastomer membrane: (a) undeformed state; (b) prestretched state; and (c) deformed state. The dot in each state denotes the position of a particular material particle.

Let $\sigma_1(R,t)$ be the true longitudinal nominal stress, and $\sigma_2(R,t)$ the true latitudinal nominal stress. Considering that the viscoelastic relaxation time of the elastomer is usually much larger than the time scale set by the inertial effect of the membrane, we neglect the inertial effect in our analysis. For quasi-static equilibrium processes, force balance in z-direction gives that

$$-\frac{1}{R}\frac{\partial}{\partial R}\left(\frac{\sigma_1}{\lambda_1}R\sin\theta\right)+\lambda_1\lambda_2\frac{p}{H}\cos\theta=0 \tag{3}$$

and force balance in latitudinal direction gives that

$$\frac{1}{R}\frac{\partial}{\partial R}\left(\frac{\sigma_1}{\lambda_1}R\cos\theta\right)-\frac{\sigma_2}{R\lambda_2}+\lambda_1\lambda_2\frac{p}{H}\sin\theta=0. \tag{4}$$

In the electrical equilibrium state, the voltage between the two electrodes equals to the voltage of the source Φ, and the electric field is $E=(\Phi\lambda_1\lambda_2)/H$.

Then we consider the boundary conditions. At the edge, the membrane is clamped. That is,

$$r(A,t)=a,\quad z(A,t)=0. \tag{5}$$

The membrane will deform into axisymmetric shape and the symmetry requires that

$$\theta(0,t)=0,\quad r(0,t)=0. \tag{6}$$

III. VISCOELASTIC MODEL OF DIELECTRIC ELASTOMER MEMBRANE

The viscoelastic behavior of the dielectric elastomer membrane is represented by a rheological model of springs and dashpots. Here, we adopt a rheological model of two parallel units:[26] one unit consists of a spring of the shear modulus μ_α and the other unit consists of a spring of the shear modulus μ_β and a dashpot of the viscosity η (Fig. 2). By employing this rheological model, the two stretches of the dielectric elastomer membrane λ_1 and λ_2 are assumed to be the net stretches of both units. Let ξ_1 and ξ_2 be the stretches in the dashpot. Then the stretches of the spring which is connected to the dashpot in series can be determined as $\lambda_1^e=\lambda_1\xi_1^{-1}$ and $\lambda_2^e=\lambda_2\xi_2^{-1}$. Treat ξ_1 and ξ_2 as two internal variables. By employing the non-equilibrium thermodynamic theory[26,30] and the neo-Hookean material model, the viscoelasticity model of the dielectric elastomer can be written as

$$\begin{aligned}\sigma_1+\varepsilon E^2&=\mu_\alpha(\lambda_1^2-\lambda_1^{-2}\lambda_2^{-2})+\mu_\beta(\lambda_1^2\xi_1^{-2}-\xi_1^2\xi_2^2\lambda_1^{-2}\lambda_2^{-2}),\\ \sigma_2+\varepsilon E^2&=\mu_\alpha(\lambda_2^2-\lambda_1^{-2}\lambda_2^{-2})+\mu_\beta(\lambda_2^2\xi_2^{-2}-\xi_1^2\xi_2^2\lambda_1^{-2}\lambda_2^{-2}),\end{aligned} \tag{7}$$

$$\begin{aligned}\frac{1}{\xi_1}\frac{\mathrm{d}\xi_1}{\mathrm{d}t}&=\frac{1}{3\eta}\left[\mu_\beta(\lambda_1^2\xi_1^{-2}-\xi_1^2\xi_2^2\lambda_1^{-2}\lambda_2^{-2})\right.\\ &\quad\left.-\frac{\mu_\beta}{2}(\lambda_2^2\xi_2^{-2}-\xi_1^2\xi_2^2\lambda_1^{-2}\lambda_2^{-2})\right],\\ \frac{1}{\xi_2}\frac{\mathrm{d}\xi_2}{\mathrm{d}t}&=\frac{1}{3\eta}\left[\mu_\beta(\lambda_2^2\xi_2^{-2}-\xi_1^2\xi_2^2\lambda_1^{-2}\lambda_2^{-2})\right.\\ &\quad\left.-\frac{\mu_\beta}{2}(\lambda_1^2\xi_1^{-2}-\xi_1^2\xi_2^2\lambda_1^{-2}\lambda_2^{-2})\right].\end{aligned} \tag{8}$$

In Eq. (7), ε is the permittivity of the dielectric elastomer membrane and εE^2 is the Maxwell stress. From Eqs. (7) and (8), we can conclude that, except of the permittivity ε, all the material parameters of the dielectric elastomer can be measured by routine mechanical tests, such as uniaxial creep or relaxation, which is the consequence of ideal dielectric elastomer assumption.[3]

In the presented model, the rate of deformation in the dashpot is described by the two components $\xi_1^{-1}\mathrm{d}\xi_1/\mathrm{d}t$ and $\xi_2^{-1}\mathrm{d}\xi_2/\mathrm{d}t$ and the dashpot is modeled as Newtonian fluid. It is noted here that this kinetic model satisfies the thermodynamic inequality if $\eta>0$.

In this article, we focus on the viscoelastic relaxation of the dielectric elastomer subject to a combination of pressure and voltage. To simplify the problem, without losing any significance, we assume that the time scale for the prestretch process is much shorter than the characteristic time of material relaxation. Under this assumption, we have the initial conditions as

$$\xi_1(R,0)=1,\quad \xi_2(R,0)=1. \tag{9}$$

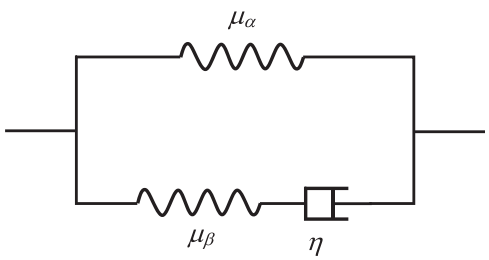

FIG. 2. Viscoelastic model of the dielectric elastomer.

Equation (9) means that at the initial time $t = 0$, the load is carried by both springs and the dashpot does not deform. This assumption is true for the elastomers having long relaxation time but might not be precise for the elastomers having short relaxation time.

IV. NOTES ON SOLVING TECHNIQUE

The governing equations presented in Secs. II and III can be rewritten into two sets. The first set is a system of first-order ordinary differential equations with respect to spatial coordinate R for the four functions: $r(R,t)$, $z(R,t)$, $\theta(R,t)$, and $\lambda_1(R,t)$ and the second set is a system of first-order ordinary differential equations with respect to time t for the two functions: $\xi_1(R,t)$ and $\xi_2(R,t)$. A combination of Eqs. (3) and (4) along with Eq. (7) gives

$$\frac{d\theta}{dR} = -\frac{\sigma_2}{\sigma_1}\frac{\lambda_1}{\lambda_2}\frac{\sin\theta}{R} + \frac{\lambda_1^2\lambda_2}{\sigma_1}\frac{p}{H}, \tag{10}$$

$$\frac{d\lambda_1}{dR} = \frac{1}{f_1}\times\left[\frac{1}{R}\left(\frac{\sigma_2}{\lambda_2}\cos\theta - \frac{\sigma_1}{\lambda_1}\right) - \frac{f_2}{R}(\lambda_1\cos\theta - \lambda_2) + f_3\frac{d\xi_1}{dR} + f_4\frac{d\xi_2}{dR}\right], \tag{11}$$

where

$$\begin{aligned} f_1 &= \mu_\alpha(1 + 3\lambda_1^{-4}\lambda_2^{-2}) + \mu_\beta(\xi_1^{-2} + 3\lambda_1^{-4}\lambda_2^{-2}\xi_1^2\xi_2^2) - \varepsilon E^2\lambda_1^{-2},\\ f_2 &= 2[\lambda_1^{-3}\lambda_2^{-3}(\mu_\alpha + \mu_\beta\xi_1^2\xi_2^2) - \varepsilon E^2\lambda_1^{-1}\lambda_2^{-1}],\\ f_3 &= 2\mu_\beta(\lambda_1\xi_1^{-3} + \lambda_1^{-3}\lambda_2^{-2}\xi_1\xi_2^2),\\ f_4 &= 2\mu_\beta\lambda_1^{-3}\lambda_2^{-2}\xi_1^2\xi_2. \end{aligned} \tag{12}$$

Equations (1), (2), (10), and (11) construct the first set of the first-order ordinary differential equations. Rewriting Eq. (8), we obtain the second set of the first-order ordinary differential equations as

$$\begin{aligned} \frac{\mathrm{d}\xi_1}{\mathrm{d}t} &= \frac{1}{3\eta}\left[\mu_\beta(\lambda_1^2\xi_1^{-1} - \xi_1^3\xi_2^2\lambda_1^{-2}\lambda_2^{-2}) - \frac{\mu_\beta}{2}(\lambda_2^2\xi_1\xi_2^{-2} - \xi_1^3\xi_2^2\lambda_1^{-2}\lambda_2^{-2})\right],\\ \frac{\mathrm{d}\xi_2}{\mathrm{d}t} &= \frac{1}{3\eta}\left[\mu_\beta(\lambda_2^2\xi_2^{-1} - \xi_1^2\xi_2^3\lambda_1^{-2}\lambda_2^{-2}) - \frac{\mu_\beta}{2}(\lambda_1^2\xi_1^{-2}\xi_2 - \xi_1^2\xi_2^3\lambda_1^{-2}\lambda_2^{-2})\right]. \end{aligned} \tag{13}$$

By using the initial conditions (9), we can determine all the physical fields at $t_0 = 0$ from the first set of the first-order ordinary differential equations by using the numerical shooting method.[31] By choosing a proper time step Δt, the stretches in the dashpot ξ_1 and ξ_2 at the next time step $t_1 = t_0 + \Delta t$ can be obtained from Eq. (13) by using the improved Euler method. Subsequently, the physical fields at the present time step t_1 can be completely determined from the first set of the first-order ordinary differential equations by using the shooting method. Repeating this procedure by continuously increasing the time, all the physical fields can be determined step by step.

V. RESULTS AND DISCUSSION

Two examples are presented in this section to illustrate the viscoelastic behaviors of the dielectric elastomer membrane when subject to pressure and voltage. In the calculation, we assume that there is no prestretch in the dielectric elastomer, namely $a/A = 1$. We also set $\mu_\alpha = \mu_\beta = \mu/2$. To plot the results, we normalize the pressure as $p/(\mu H/A)$, the voltage as $\Phi/H/(\mu/\varepsilon)^{1/2}$, the coordinate as R/A, and the time as t/t_v. Here, $t_v = \eta/\mu_\beta$ is known as the viscoelastic relaxation time.

We first consider the case that the dielectric elastomer membrane is only subject to pressures. Figs. 3(a)–3(d) plot the evolution of the longitudinal stretch λ_1, the apical height z, the longitudinal true stress σ_1, and the stretch in the dashpot ξ_1, at the center of the membrane, when it is subject to different pressures while the voltage keeps zero. At the short-time limit, the deformation of the dashpot in Fig. 2 is zero and the elastic properties of the dielectric elastomer can be represented by two parallel springs; at the long-time limit, the spring connected with the dashpot is fully relaxed and the stress in it is zero. The elastic properties of the dielectric elastomer can be represented by a single spring, μ_α in Fig. 2. It is also well known that no equilibrium state can be found when the pressure exerted on a circular neo-Hookean membrane is beyond a critical value compared to its modulus. Therefore, the elastomeric membrane may be stable for the short-time limit but unstable for the long-time limit, even under a constant pressure. This expected trend is illustrated in Figs. 3(a)–3(d). When the pressure is small, for example, $p/(\mu H/A) = 0.8$ and $p/(\mu H/A) = 0.9$, all the physical quantities finally evolve into constant values. For example, under the pressure $p/(\mu H/A) = 0.9$, both the longitudinal and latitudinal stretches change little when $t/t_v > 20$. However, when the pressure is large, the elastomeric membrane is initially stable but become unstable with the evolution. For instance, mechanical equilibrium state cannot be found in the membrane for $p/(\mu H/A) = 1.0$ when $t/t_v > 12$, which indicates the membrane lose mechanical stability after a certain period of evolution. In practice, considering the membrane is made of VHB with $t_v = 65.5$ s,[32] we predict that the membrane will become unstable after 786 s under the pressure $p/(\mu H/A) = 1.0$. To confirm our calculated results, we also plot both short-time limit and long-time limit in Figs. 3(a)–3(d) by using different methods described in Ref. 7.

In Fig. 4, we plot the distributions of the longitudinal and latitudinal stretches at several different times with two different pressures $p/(\mu H/A) = 0.9$ and 1.0. In the whole evolution process, both longitudinal and latitudinal stretches increase with time and the largest stretches appear at the apex of the membrane. Fig. 5 shows the deformed shapes of the membrane at different times when subjected to $p/(\mu H/A) = 0.9$ and 1.0, respectively. The deformation and the shape of the membrane evolve dramatically faster, under the pressure $p/(\mu H/A) = 1.0$ and the membrane finally loses mechanical stability.

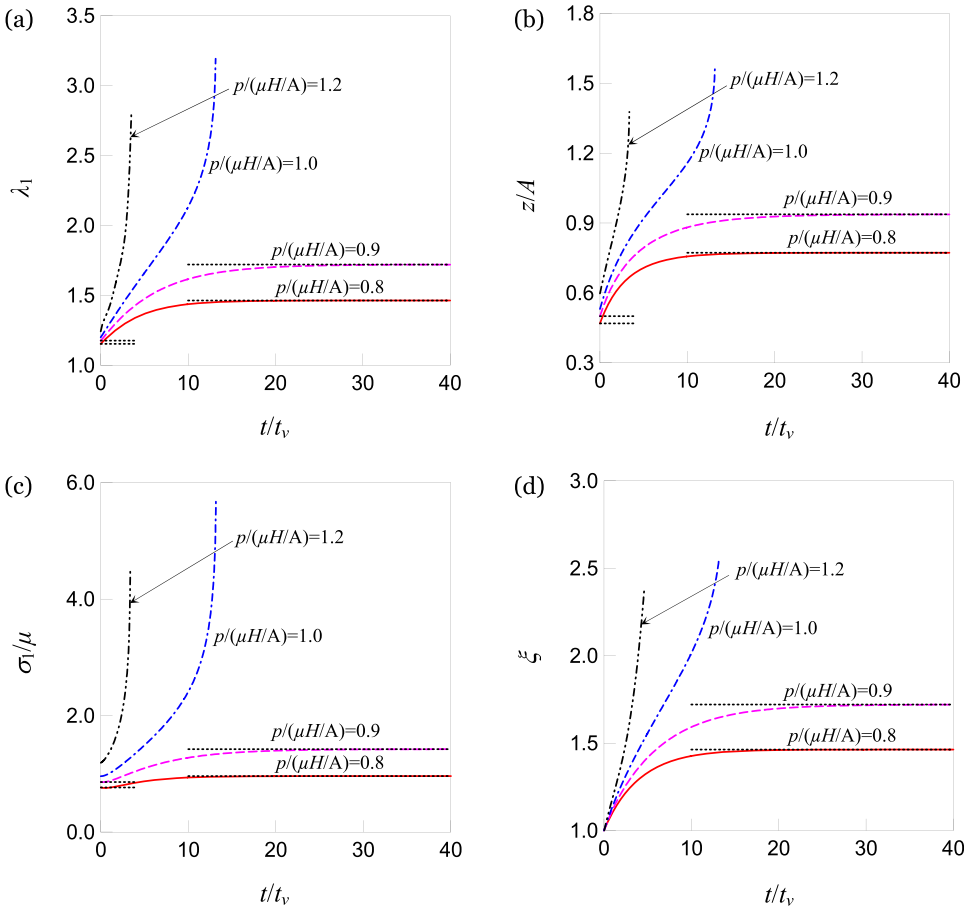

FIG. 3. Evolution of (a) longitudinal stretch, (b) apical height, (c) true stress, and (d) stretch of the dashpot at the center of the membrane under several different pressures. In the figure, horizontal dash lines represent equilibrium solutions for short-time limit and long-time limit.

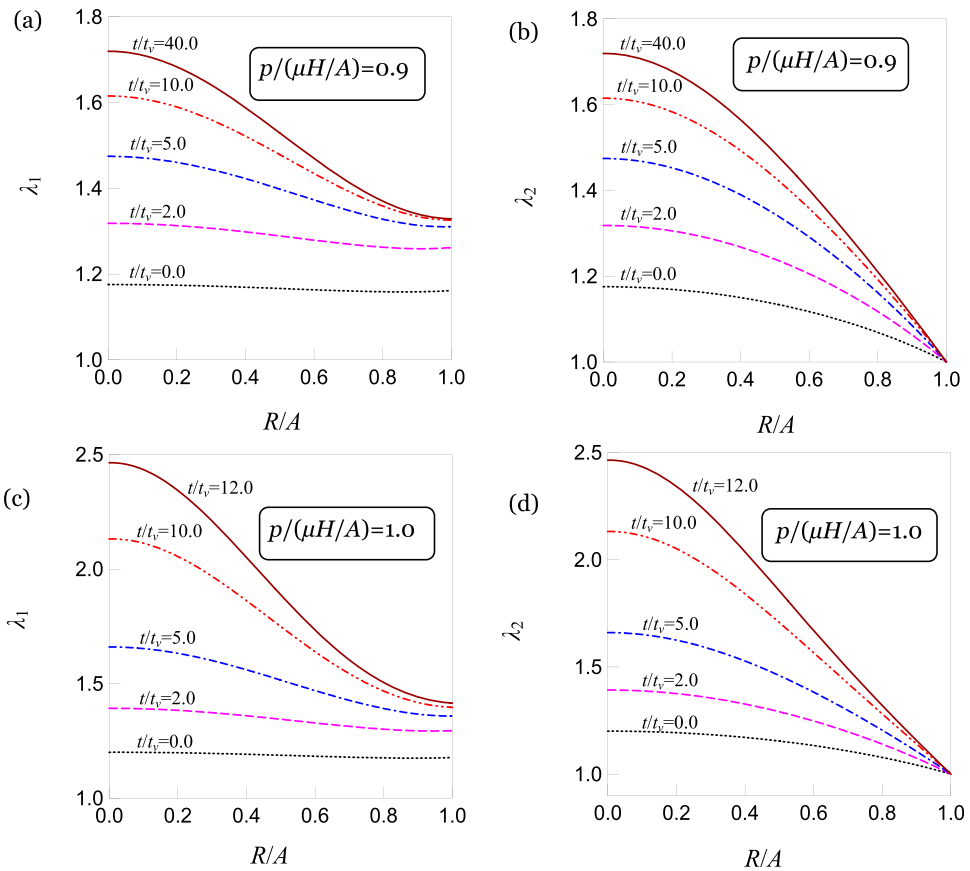

FIG. 4. Evolution of longitudinal stretch and latitudinal stretch in the dielectric elastomer membrane with the two different pressures.

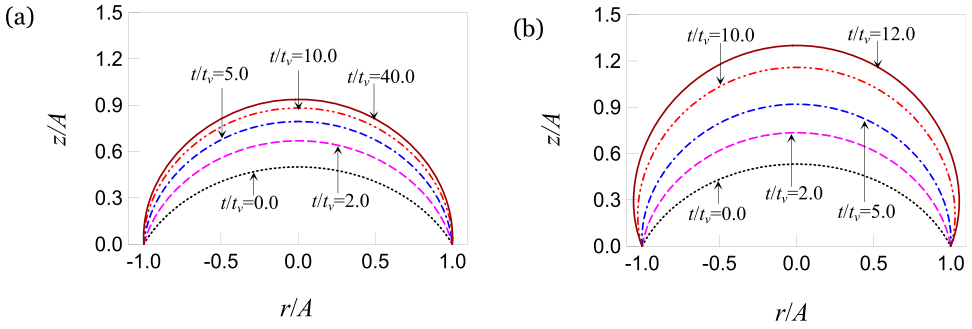

FIG. 5. Evolution of the shape of the soft dielectric membrane with two different pressures (a) $p/(\mu H/A) = 0.9$. (b) $p/(\mu H/A) = 1.0$.

The second example studied here is the dielectric membrane subject to different voltages Φ while the pressure keeps constant $p/(\mu H/A) = 0.5$. Figure 6 plots the evolution of the longitudinal stretch λ_1, the apical height z, the longitudinal true stress σ_1, and the true electric field E at the center of the membrane. Similarly, for small voltages, for example, $\Phi/H/(\mu/\varepsilon)^{1/2} = 0.1$ and 0.2, all the physical quantities finally evolve into equilibrium values, while for larger voltages, $\Phi/H/(\mu/\varepsilon)^{1/2} = 0.3$ and 0.4, no electromechanical equilibrium state can be found after a period of time. Figure 6(c) shows that the true longitudinal stress at the center is not a monotonic increasing function of the time. This may be due to the electromechanical coupling effect in the dielectric elastomer membrane.

Fig. 7 plots the distribution of longitudinal and latitudinal stretches of the dielectric elastomeric membrane at several different times, when the applied voltage $\Phi/H/(\mu/\varepsilon)^{1/2} = 0.2$ and 0.3, respectively. Subject to the voltage $\Phi/H/(\mu/\varepsilon)^{1/2} = 0.2$, the dielectric elastomeric membrane approaches electromechanical equilibrium state when $t/t_v > 20$, while no electromechanical equilibrium state can be found for $\Phi/H/(\mu/\varepsilon)^{1/2} = 0.3$ when $t/t_v > 20$.

Figure 8 shows the deformed shapes of the membrane at different times when the membrane is subject to $\Phi/H/(\mu/\varepsilon)^{1/2} = 0.2$ and 0.3, respectively. It shows that at the same time, the membrane under $\Phi/H/(\mu/\varepsilon)^{1/2} = 0.3$ has a much larger apical height than that under $\Phi/H/(\mu/\varepsilon)^{1/2} = 0.2$. When the applied voltage $\Phi/H/(\mu/\varepsilon)^{1/2} = 0.2$, the shape of the dielectric elastomeric membrane changes little from $t/t_v = 10$ to $t/t_v = 40$. When the applied voltage $\Phi/H/(\mu/\varepsilon)^{1/2} = 0.3$, the shape of the dielectric elastomeric membrane changes very dramatically from $t/t_v = 10$ to $t/t_v = 20$. After $t/t_v = 22$, no electromechanical equilibrated shape of the dielectric membrane can be found.

Recently, viscoelastic deformations of dielectric elastomer under electromechanical loads have been clearly observed in a

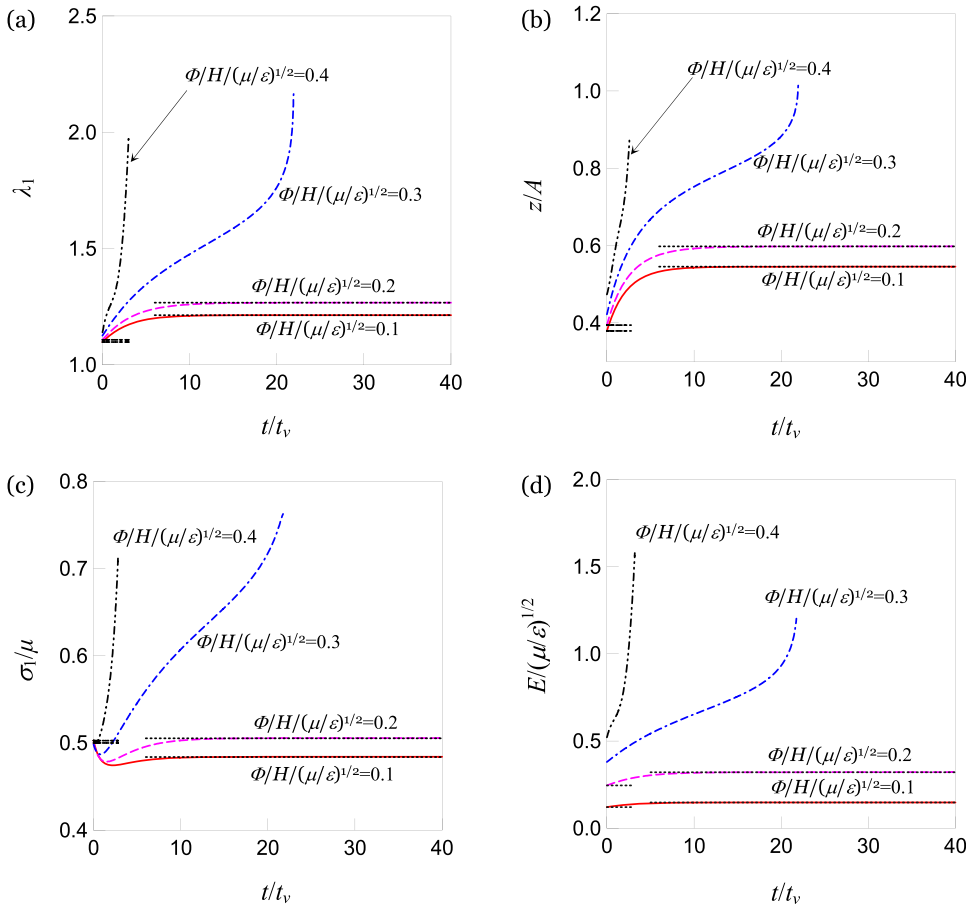

FIG. 6. Evolution of (a) longitudinal stretch, (b) apical height, (c) true stress, and (d) electric filed at the center of the membrane under several different voltages, while the pressure is kept as a constant $p/(\mu H/A) = 0.5$. In the figure, horizontal dash lines represent equilibrium solutions for short-time limit and long-time limit.

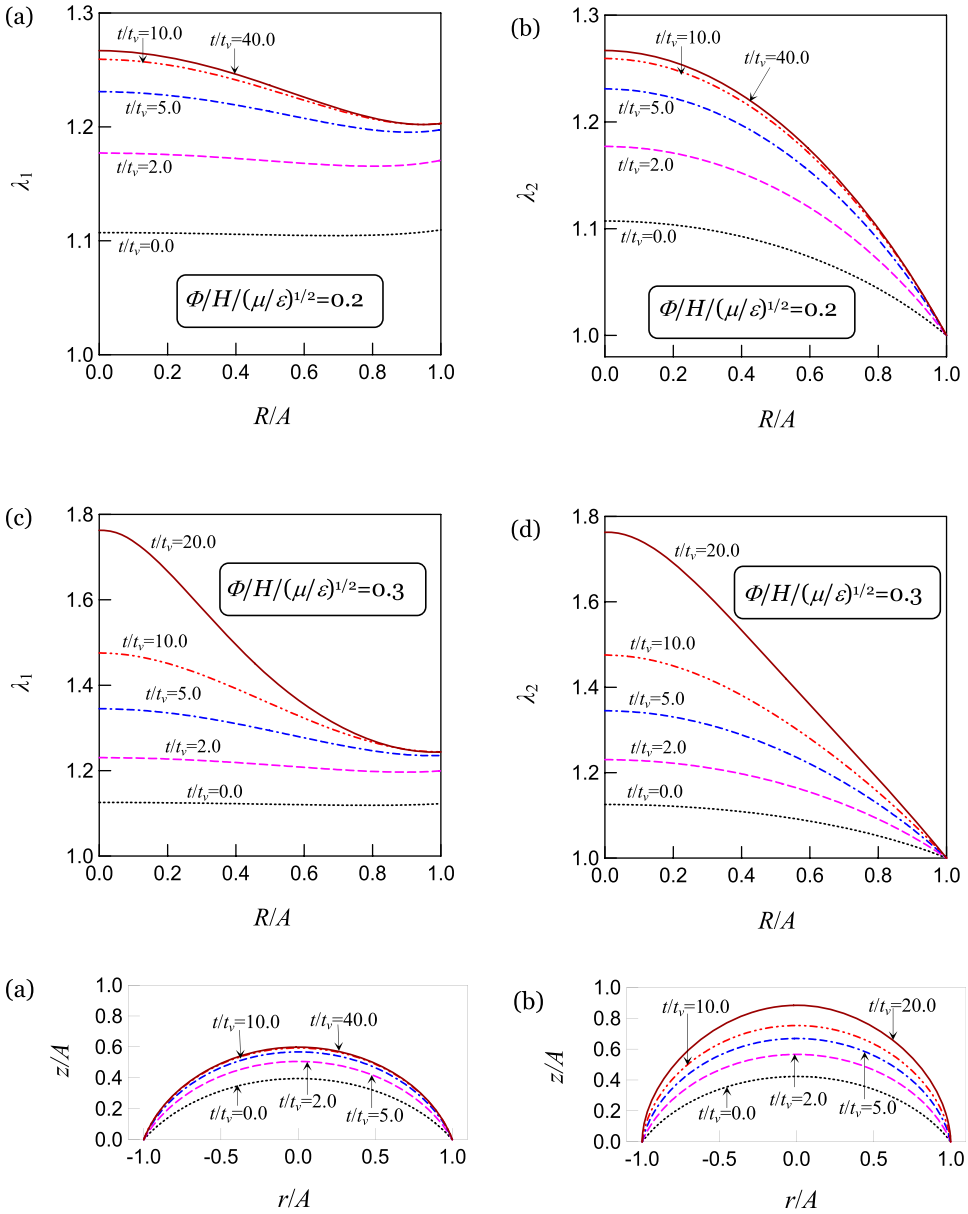

FIG. 7. Evolution of longitudinal stretch and latitudinal stretch in the dielectric elastomer membrane with the two different applied voltages.

FIG. 8. Evolution of the shape of the dielectric elastomer membrane at two different voltages (a) $\Phi/H/(\mu/\varepsilon)^{1/2} = 0.2$. (b) $\Phi/H/(\mu/\varepsilon)^{1/2} = 0.3$.

similar setup in experiments. As reported by Li *et al.*,[16] for a dielectric elastomer of acrylic elastomer mounted on a chamber of fixed volume, when the voltage is ramped up and kept at 5.5 kV for several minutes, the membrane continues deform and even form wrinkles after a while. Using the current viscoelastic model, we can possibly study the delayed wrinkling phenomenon described in Ref. 16.

VI. CONCLUSIONS

Equilibrium thermodynamic modeling of dielectric elastomers have been developed and used intensively to analyze the performance of various dielectric elastomeric structures. While viscous relaxations in dielectric elastomers have been often observed in experiments, few theoretical analysis can be found in modeling large and inhomogeneous deformations in dielectric elastomers with considering the effect of viscoelasticity. In this article, we study the viscoelastic deformation in a circular dielectric elastomer membrane subject to pressure and voltage. The evolution of various physical fields in the membrane has been calculated. We further show that when the pressure or voltage is small, the dielectric elastomer can evolve to an equilibrium state after a certain time. However, if the pressure or voltage is beyond a critical value, no equilibrium state can be reached. The calculation results may help to understand some time-dependent failure modes observed in dielectric elastomer structures. It should also be pointed out that the analysis in this paper is based on the neo-Hookean material model. The stiffening effect of the elastomeric membranes at large deformation is ignored. To study the stiffening effect, further investigations can be performed by replacing the neo-Hookean model in the current by the material models considering the stiffening effect, such as Gent model[33] and Arruda-Boyce model.[34]

ACKNOWLEDGMENTS

This work at Zhejiang University was supported by Key Team of Technological Innovation of Zhejiang Province (Grant 2011R09025-05), the Zhejiang Provincial Natural

Science Foundation of China (No. LY13A020001), and by the Fundamental Research Funds for the Central Universities (No. 2011XZZX002). Shengqiang Cai acknowledges the startup funds from the Jacobs School of Engineering at University of California, San Diego.

[1]R. Pelrine, R. Kornbluh, Q. B. Pei, and J. Josepch, Science **287**, 836 (2000).
[2]A. O'Halloran, F. O'Malley, and P. McHugh, J. Appl. Phys. **104**, 071101 (2008).
[3]Z. G. Suo, Acta Mech. Solida Sinica **23**, 549 (2010).
[4]N. Goulbourne, E. Mockensturm, and M. Frecker, ASME J. Appl. Mech. **72**, 899 (2005).
[5]J. W. Fox and N. C. Goulbourne, J. Mech. Phys. Solids **56**, 2669 (2008).
[6]J. W. Fox and N. C. Goulbourne, J. Mech. Phys. Solids **57**, 1417 (2009).
[7]J. Zhu, S. Q. Cai, and Z. G. Suo, Int. J. Solids Struct. **47**, 3254 (2010).
[8]X. H. Zhao and Z. G. Suo, Phys. Rev. Lett. **104**, 178302 (2010).
[9]L. W. Liu, Y. J. Liu, J. S. Leng, and K. T. Lau, Smart Mater. Struct. **20**, 115015 (2011).
[10]H. M. Wang, S. Q. Cai, F. Carpi, and Z. G. Suo, ASME J. Appl. Mech. **79**, 031008 (2012).
[11]C. Keplinger, T. F. Li, R. Baumgartner, Z. G. Suo, and S. Bauer, Soft Matter **8**, 285 (2012).
[12]T. Q. Lu, J. S. Huang, C. Jordi, G. Kovacs, R. Huang, D. R. Clarke, and Z. G. Suo, Soft Matter **8**, 6167 (2012).
[13]I. A. Anderson, T. A. Gisby, T. G. McKay, B. M. O'Brien, and E. P. Calius, J. Appl. Phys. **112**, 041101 (2012).
[14]L. W. Liu, Y. J. Liu, and J. S. Leng, J. Appl. Phys. **112**, 033519 (2012).
[15]J. S. Huang, T. F. Li, C. C. Foo, J. Zhu, D. R. Clarke, and Z. G. Suo, Appl. Phys. Lett. **100**, 041911 (2012).
[16]T. Li, C. Keplinger, R. Baumgartner, S. Bauer, W. Yang, and Z. Suo, J. Mech. Phys. Solids **61**, 611 (2013).
[17]R. Shankar, T. K. Ghosh, and R. J. Spontak, Soft Matter **3**, 1116 (2007).
[18]F. Carpi, G. Frediani, S. Turco, and D. D. Rossi, Adv. Funct. Mater. **21**, 4152 (2011).
[19]S. J. A. Koh, X. H. Zhao, and Z. G. Suo, Appl. Phys. Lett. **94**, 262902 (2009).
[20]J. Maas and C. Graf, Smart Mater. Struct. **21**, 064006 (2012).
[21]F. Carpi, S. Bauer, and D. D. Rossi, Science **330**, 1759 (2010).
[22]P. Chakraborti, H. A. K. Toprakci, P. Yang, N. D. Spigna, P. Franzon, and T. Ghosh, Sens. Actuators, A **179**, 151 (2012).
[23]J. S. Plante and S. Dubowsky, Int. J. Solids Struct. **43**, 7727 (2006).
[24]V. L. Tagarielli, R. Hildick-Smith, and J. E. Huber, Int. J. Solids Struct. **49**, 3409 (2012).
[25]M. Pharr, J. Y. Sun, and Z. G. Suo, J. Appl. Phys. **111**, 104114 (2012).
[26]C. C. Foo, S. Q. Cai, S. J. A. Koh, S. Bauer, and Z. G. Suo, J. Appl. Phys. **111**, 034102 (2012).
[27]C. C. Foo, S. J. A. Koh, C. Keplinger, R. Kaltseis, S. Bauer, and Z. G. Suo, J. Appl. Phys. **111**, 094107 (2012).
[28]T. F. Li, S. X. Qu, and W. Yang, J. Appl. Phys. **112**, 034119 (2012).
[29]J. S. Plante and S. Dubowsky, Sens. Actuators, A **137**, 96 (2007).
[30]X. H. Zhao, S. J. A. Koh, and Z. G. Suo, Int. J. Appl. Mech. **3**, 203 (2011).
[31]D. G. Zill, *A First Course in Differential Equations with Modeling Applications*, 7th ed. (Brooks/Cole, California, 2001), p. 436.
[32]S. Michel, X. Q. Zhang, M. Wissler, C. Löwe, and G. Kovacs, Polym. Int. **59**, 391 (2009).
[33]A. N. Gent, Rubber Chem. Technol. **69**, 59 (1996).
[34]E. M. Arruda and M. C. Boyce, J. Mech. Phys. Solids **41**, 389 (1993).